SUPPORTING INFORMATION

The Application of Black Silicon for Nanostructure-Initiator Mass Spectrometry

Jian Gao,[1,2] Markus de Raad,[1,2] Benjamin P. Bowen,[1,2] Ronald N. Zuckermann,[3] Trent R. Northen*,[1,2]

[1]Life Sciences Division, Lawrence Berkeley National Laboratory, 1 Cyclotron Road, Berkeley, CA 94720, USA
[2]Joint Genome Institute, Department of Energy, 2800 Mitchell Drive, Walnut Creek, CA 94598, USA
[3]The Molecular Foundry, Lawrence Berkeley National Laboratory, 1 Cyclotron Road, Berkeley, CA 94720, USA

*E-mail: TRNorthen@lbl.gov (Trent R. Northen)

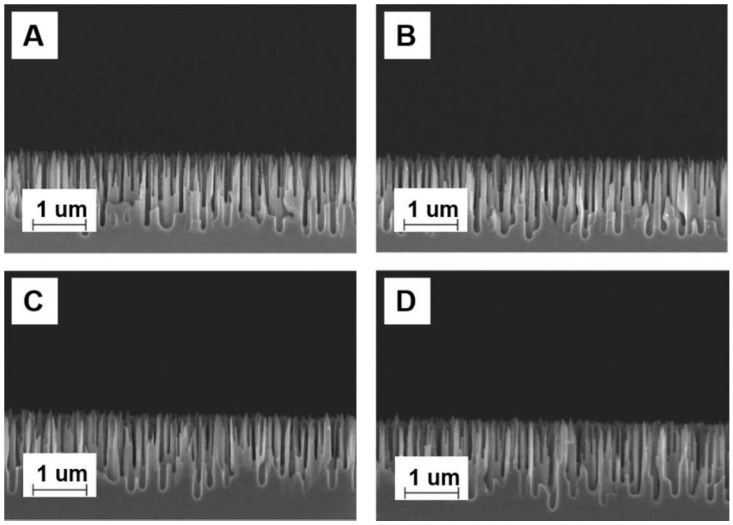

SI. 1 SEM images with cross-sectional view of four replicates of black silicon surfaces obtained at same etching condition: SF_6/O_2 30/20 sccm/sccm, -80 °C, 6.5 min. It proves the consistent surface morphologies of black silicon once etching condition is fixed.

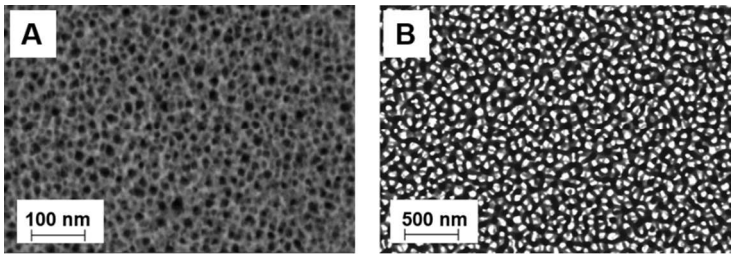

SI. 2 SEM images with top views of NIMS substrates obtained by A) HF electrochemical etching, B) SF_6/O_2 ICP etching.

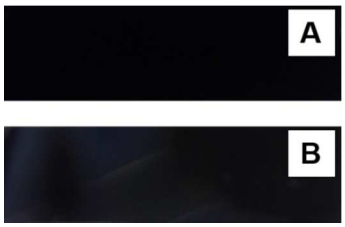

SI. 3 The photos of a black silicon NIMS substrate A) before and B) after thermal heating. The initiator film starts forming by tracking the bluish color in the second photo, which confirms initiators come out of surface with heating.

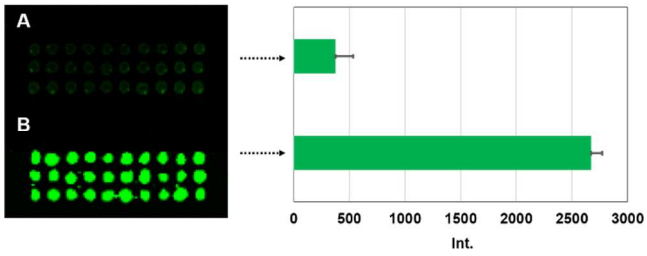

SI. 4 The sensitivity comparison of black silicon as mass spectrometry substrates: A) no initiator coating and B) with initiator coating. Palmitoylcarnitine is used as analyte, and its averaged signal intensity detected from the initiator-coated substrate is one order of magnitude higher than the signal from the uncoated substrate.

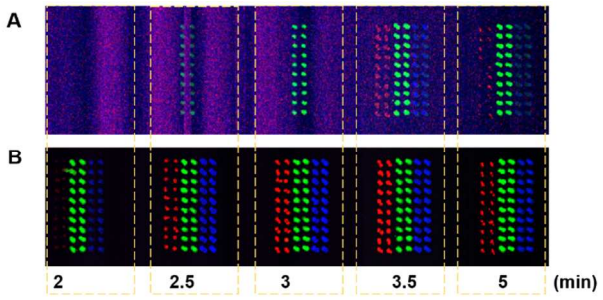

SI.5 Laser intensity dependent NIMS imaging. Panel A shows the NIMS image collected under 2000 laser power while panel B shows the image collected at 3000 laser power. Arginine is labeled in red, palmitoylcarnitine is in green, and bradykinin in blue traces. The signal is dramatically improved under high laser power, which demonstrates surface restructuring is essential to gas phase ion generation.

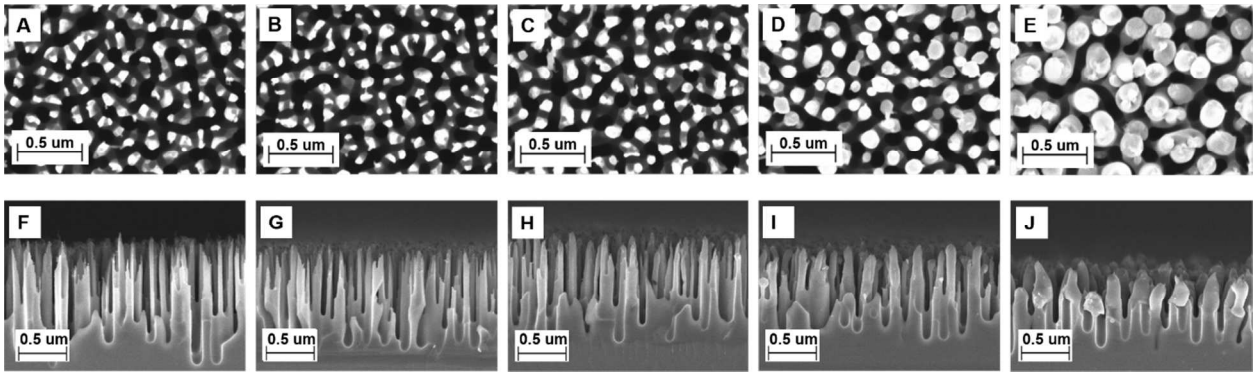

SI. 6 Laser ablation of black silicon surfaces under laser power 0, 3000, 4000, 5000, 6000. SEM images A, B, C, D and E show the top views, respectively. F, G, H, I and J show their relative SEM images in cross sectional views. Note that in general ion detection increases dramatically between 3000 and 4000 laser intensity, which is the threshold for surface rearrangement.

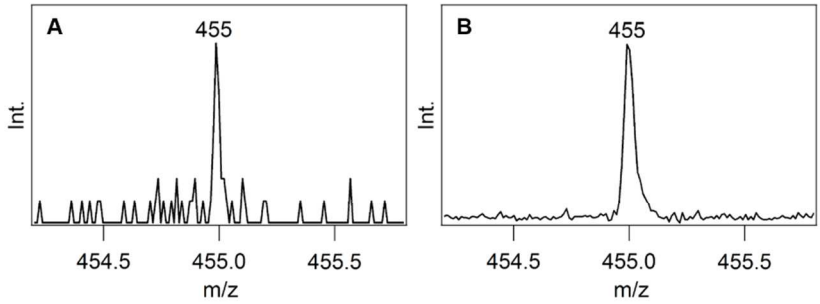

SI. 7 Mass spectra of 500 yactomole verapamil spotted on porous silicon NIMS substrates. Spectrum A is collected with one single shot laser and spectrum B is accumulated from 30 single spectra.

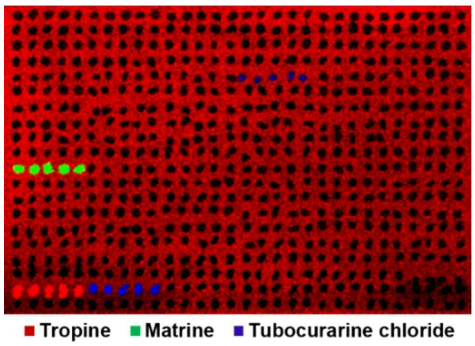

SI. 8 shows the NIMS imaging results of a library containing 118 secondary metabolites. Each compound was printed with 5 replicates at 250 fmol amount. Three compounds (tropine, matrine, tubocurarine chloride) as well as background were selected in this image to show the printed sample spot patterns. The NIMS intensities for all the compounds were listed in Table 1.

Table 1 Average signal intensity obtained using black silicon NIMS analysis of a small molecule library. [note: noise level is ~30 counts]

Compound	*m/z*	Ion Intensity [a.u.]	Compound	*m/z*	Ion Intensity [a.u.]
Spartein sulfate-5H2O	235.22	23333	Asiatic acid	489.36	–
Berberine-HCl	336.12	22901	Auraptene	299.16	–
Lappaconitine	585.32	8444	Vulpinic acid	323.09	–
Bulleyaconotine A	644.34	7895	Bergenin	329.09	–
Vindoline	457.23	6751	Cafestol	317.21	–
(+)-Tubocurarine chloride	609.30	6294	Cafestol acetate	359.22	–
Oxyacanthine sulfate	609.30	3562	Cryptotanshinone	297.15	–
Matrine	249.20	3522	4'-Demethylpipodophyllotoxin	401.12	–
Cepharanthine	607.28	3071	Mitomycin C	335.13	–
Hydrocotarnine-HBr	222.11	2150	Methysticin	275.09	–
Vinorelbine	779.40	2039	Thymoquinone	165.09	–
Corynanthine	355.20	1908	Dihydrotanshinone	279.10	–
Cephaeline-HBr	467.29	1856	Azomycin	114.03	–
_-Solanine	868.51	1692	Diosmin	609.18	–
Zerumbone	219.17	1392	Ecdysone	465.32	–
Catharanthine	337.19	1300	_-Ecdysone	481.32	–
Tropine	142.12	875	Hesperitine	303.09	–
9,10-Dihydrolysergol	257.16	856	Hesperidine	611.20	–
Evodiamine	304.14	830	Honokiol	267.14	–
Sinomenine	330.17	823	Hypocrellin A	547.16	–
Anisodamine	306.17	764	Hypocrellin B	529.15	–
Sedanolide	195.14	692	Lagochiline	357.26	–
Solasodine	414.34	679	Limonin	471.20	–
Yangonin	259.10	666	Madecassic acid	505.35	–
Ginkgolide A	409.15	568	Magnolol	267.14	–
Gelsemine-HCl	323.18	562	Minocycline-HCl	458.19	–
Rutaecarpine	288.11	529	Naringin	581.19	–
Vincamine	355.20	477	Indole-3-acetic acid	176.07	–
(±)-Anabasine	163.12	450	16-Oxocafestol	285.18	–
Salsoline	194.12	437	16-Oxokahweol	283.17	–
Salsolodine	208.13	424	Panaxadiol	461.40	–
Chlorogenic acid	355.10	405	Panaxatriol	477.39	–
Securinine	218.12	352	GERI-BP002-A	341.25	–
Senecionine	336.18	320	Pimaricin	666.31	–
Diosmetine	301.07	307	Podophyllotoxin	415.14	–

Geraldol	301.07	235	Rubescensin A	365.20	–
Formononetin	269.08	228	Rutin	611.16	–
Biochanin A	285.08	209	Santonin	247.13	–
Lupinine	170.15	196	Schisantherin A	537.21	–
5,6-Dehydrokawain	229.09	156	Silybine	483.13	–
R(+)-Schisandrin A	417.23	130	Silymarin	483.13	–
Flavokawain A	315.12	124	Solanesol	631.58	–
Harringtonine	532.25	124	Bergapten	217.05	–
(-)-Cytisine	191.12	124	Betulin	443.39	–
Galangine	271.06	124	Dihydrorobinetine	305.07	–
L-Theanine	175.11	111	Flavanomarein	451.12	–
Scopoletin	193.05	98	Lavendustin B	366.13	–
Brassinin	237.05	98	Lavendustin A	382.13	–
Coumestrol	269.04	98	Verruculogen	514.25	–
Euphorbiasteroid	553.28	84	Amphotericin B	924.50	–
S(-)-Schisandrin A	401.20	71	Amygdalin	458.17	–
Bis demethoxycurcumin	309.11	71	Aphidicolin	339.25	–
Xanthotoxin	217.05	65	Arbutin	273.10	–
Diindolylmethane	247.12	65	Sclerotiorin	391.13	–
Salinomycin	751.50	–	Bleomycin sulfate	1414.52	–
Digitoxin	765.44	–	Chartreusin	641.19	–
Myristicin	193.09	–	Ferulic acid	195.07	–
Dicoumarol	337.07	–	Bakuchiol	257.19	–
Artemesinin	283.15	–	Indole-3-carbinol	148.08	–